Temporal changes in the slope-scale spatial variability of the shear strength of buried surface hoar layers

Spencer Logan, Karl Birkeland, Kalle Kronholm, and Kathy Hansen

In press for:

Cold Regions Science and Technology
ISSW 2004 Special Issue (to be published in 2006)

TEMPORAL CHANGES IN THE SLOPE-SCALE SPATIAL VARIABILITY OF THE SHEAR STRENGTH OF BURIED SURFACE HOAR LAYERS

Spencer Logan[1,2], Karl Birkeland[2,3], Kalle Kronholm[2], Kathy Hansen[2]

[1]Colorado Avalanche Information Center

325 Broadway St., WS#1, Boulder, CO 80305

[2]Department of Earth Sciences, Montana State University

Bozeman, MT 59717-3480 USA

[3]U. S. Forest Service National Avalanche Center, P.O. Box 130, Bozeman, MT 59771 USA

ABSTRACT: Determining whether the snowpack is becoming more spatially variable or uniform is important for accurate avalanche forecasts. Greater variability increases uncertainty in extrapolation and prediction. Our results offer a look at the evolution of the spatial variability of shear strength of two buried surface hoar layers in southwestern Montana, USA, over time. We studied the layers from shortly after burial until they were no longer the weakest layer in the snowpack. We selected study sites with planar slopes, uniform ground cover, and wind-sheltered locations. This simplified the comparison of the plots by minimizing initial spatial differences so we could focus on temporal change. Within each site, we sampled four 14 m x 14 m plots with more than 70 shear frame tests in a layout optimized for spatial analysis. At both sites, the layers gained strength at a rate that slowed as the layers aged. Although there was little change in the relative variability, absolute variability increased through time. Temporal change was more pronounced when the layers were younger and were gaining strength more rapidly. Additional tests at one plot suggested a correlation length, or the distance at which test results are related, for shear strength of just a few meters. At the other plot, the surface hoar layer collapsed during the initial sample. An initial dramatic decrease in shear strength occurred after this collapse followed by strengthening during that day and into the following day. Though we measured increasing absolute variability through time, uncovering changes in our other measures of spatial variability proved elusive. Developing methods and techniques for adequately characterizing variability, and temporal changes in that variability, will continue to be challenging.

Corresponding authors' e-mail: spencer_logan@hotmail.com
kbirkeland@fs.fed.us

KEYWORDS: spatial variability, avalanches, avalanche forecasting, temporal change

1. INTRODUCTION

Forecasting avalanche hazard requires integrating data gathered at various scales and extrapolating to areas of interest. At the scale of individual avalanche slopes, results from stability tests such as rutschblocks, compression tests, or shear frames, provide critical information. However, stability test results vary across slopes. The spatial variability affects the reliability of extrapolation by introducing uncertainty (LaChapelle, 1980; McClung, 2002). Without knowing the degree of the variability, it is difficult to assess the avalanche potential.

The shear strength of weak layers is important data for avalanche forecasting because slab avalanches initiate as shear fractures within weak layers. Persistent weak layers, which remain in the snowpack for weeks or months, are the most problematic to humans (Jamieson and Johnston, 1992; Schweizer and Jamieson, 2001). Weak layers tend to gain strength as they age, but the rate of strengthening decreases with time (Jamieson and Johnston, 1999; Jamieson and Schweizer, 2000). Experience and previous research suggest that shear strength of persistent weak layers can vary dramatically over a slope (e.g., Conway and Abrahamson, 1984; Stewart and Jamieson, 2002; Kronholm and Schweizer, 2003; Landry et al., 2004), and that slope-scale spatial variability may change through time (Birkeland and Landry, 2002). Less stable slopes may be more spatially uniform than more stable slopes (Birkeland and Landry, 2002). Kronholm and Schweizer (2003) proposed a scheme to relate variability and slope stability.

We examined the temporal changes in shear strength by concentrating on two different layers of buried surface hoar during the 2003-2004 winter, sampled on small, uniform slopes. We examined the spatial variability of shear strength on a given day, and how the spatial variability changed through time. Quantifying trends in the temporal changes of spatial variability of shear strength will improve avalanche forecasting. Knowing that stability tests were becoming more variable would allow avalanche forecasters to seek data at a greater spatial density to reduce uncertainty, or confine extrapolation to shorter distances. Conversely, if stability tests become less spatially variable, reliable extrapolation would be possible over greater distances.

2. METHODS

The two study sites are located in southwestern Montana, USA (Figure 1). They are in the intermountain avalanche climate zone which exhibits a variety of avalanche and snowpack conditions, including persistent weak layers (Mock and Birkeland, 2000; Tremper, 2001). As different parts of a site were sampled at different times, we selected the sites to minimize sources of variability across the site, such as wind drifting, changes in slope angle, substrate, and shrubs. Signs placed at the beginning of the winter kept each site undisturbed by skiers.

The Spanky's site is 3.5 km north of Big Sky, Montana USA (45° 19.3' N 111° 22.7' W), in a wind-sheltered glade with an east-northeast aspect at an elevation of 2640 m. The average slope angle is 27° and the soil surface varies less than 5° in angle or aspect. Vegetation ranges from grass and forbs to shrubs 0.4 m high. When sampled, the surface hoar layer was more than 1 m above the ground.

The Lionhead site is located 17 km west of West Yellowstone, Montana USA (44° 42.2' N 111° 17.6' W), in a glade with a northeast aspect at an elevation of 2340 m. The average slope angle is 27° with 6° of variation across the site. There are more shrubs than the Spanky's site, but the shrubs were no taller. The surface hoar layer was more than 1 m above the ground when sampled. The nearest tree was located 2 m below the lower left corner of the site.

2.1. Site Layout and Sampling

Each site consisted of four 14 m x 14 m plots in two rows, separated by 3 m wide alleys. The alleys, sampled first, allowed us to investigate any initial site-scale trends or patterns. The alleys consisted of 48 shear frame tests in 12 pits of four tests. Test centers were 0.5 m apart. Slab thickness and density were measured at each pit (Figure 2).

We sampled the first plot within a few days of the alleys, and the subsequent plots at approximately weekly intervals. We chose sample days to follow periods of snowfall and to allow for sufficient changes in shear strength. In each plot, we grouped 74 shear frame tests into five main pits of 10-12 tests and four smaller pits of four tests each. The five main pits allowed for pit-to-pit and pit-to-plot comparisons (Birkeland and Landry, 2002; Landry, 2002, Landry et al., 2004). The four smaller

pits improved calculations of spatial statistics. Within each pit, test centers were 0.5 m apart. Slab thickness and density were measured at all nine pits. A manual study profile and rutschblock (Greene et al., 2004) was conducted adjacent to the first pit sampled.

We utilized shear frame tests to quantify shear strength of the buried surface hoar layers (Jamieson and Johnston, 2001). Shear frames allowed the targeting of a specific weak layer, even when it was no longer the weakest layer in the snowpack, so we were able to sample the same layer in all four plots. All tests used standard 0.025 m^2 frame, and the same operator conducted all tests at a site. Size corrected shear strength (τ_∞) was calculated by

$$\tau_\infty = 0.65 \frac{F_{fail}}{A_{frame}} \quad (1)$$

where F_{fail} is the force at failure in newtons, A_{frame} the frame area, and 0.65 a correction for frame area (Föhn, 1987).

2.2. Analysis

Two statistical descriptors described the plot data: the median to describe central tendency, and the quartile coefficient of variation (QCV), a robust measure of the relative spread of the data. The QCV and is defined as:

$$QCV = \frac{(Q3 - Q1)}{(Q3 + Q1)} \quad (2)$$

where Q1 and Q3 are the first and third quartiles, respectively. The QCV is similar to, but not equivalent to, a parametric coefficient of variation (CV) (Spiegel and Stephens, 1999). The CV can be approximated by CV = 3/2 * QCV (Spiegel and Stephens, 1999). In general, we used non-parametric statistics because the distributions of shear strength failed the Kolmogorov test for normalcy on Spanky's Plots 2, 3, and 4, and Lionhead Plot 3. However, to compare variances between days we used a T-test, which was appropriate since our sample size was sufficiently large (N > 122) (Neter et al., 1996).

Trend surfaces used to analyze any plot-wide trends, *t(s)*, and variograms were used to analyze spatial autocorrelation within the residuals, ε(s) (Cressie, 1993; Kronholm 2004), so that the value at a location *s* = (x,y) was

$$Z(\mathbf{s}) = t(s) + \varepsilon(s) \tag{3}$$

The large-scale trend, *t(s)*, was composed of slope in the X and Y directions, $a_2(x)$ and $a_3(y)$ respectively, and the intercept, a_1, such that

$$t(s) = a_1 + a_2(x) + a_3(y). \tag{4}$$

The trend was removed if it was significant ($p < 0.05$) and explained more than 10% of the variability in the data ($R^2 > 0.10$) (Birkeland et al., 2004). If the trend explained less than 10% of the variability, it had little discernable effect on the subsequent variogram analysis and was not removed (Logan, 2005). Using linear trends did not imply that trends present in the snowpack were actually linear. Linear trends provided a better fit than higher order trend surfaces, and were relatively easy to interpret (Logan, 2005).

Variograms quantify the spatial autocorrelation within a data set by calculating the average variance between data points over distance and explicitly include measurement location (Webster and Oliver, 2001). Only recently have variograms been applied to shear strength and stability data (e. g. Kronholm, 2004; Logan 2005), although variograms have been applied to other snowpack properties such as depth or snow water equivalent (Blöschl, 1999).

After comparing the performance of the classical and several robust variograms (Lark, 2000; Logan, 2005), the Cressie and Hawkins robust variogram (Cressie, 1993, p. 75) was selected because outliers were given less weight in the calculations, and results were less influenced by non-normal data. In the Cressie and Hawkins robust variogram estimator, the semivariance, *γ(h)*, was defined as

$$\gamma(h) = \frac{\left\{ \frac{1}{|N(h)|} \sum_{N(h)} \left| Z(s_i) - Z(s_{i+h}) \right|^{1/2} \right\}^4}{2\left(0.457 + \frac{0.049}{|N(h)|} \right)}, \tag{5}$$

where $Z(s_i)$ and $Z(s_{i+h})$ are the values at locations separated by the distance *h*, and *N(h)* is the number of point-pairs separated by that distance (Cressie, 1993).

The variogram range was the distance at which the data was no longer autocorrelated and represented the limits of spatial dependence (Webster and Oliver, 2001). The variogram nugget was variance at h = 0, and indicated variability that could not be resolved by the spatial structure (Webster and Oliver, 2001). Nuggets may have several causes, ranging from lack of data at shorter distances, to inherent variability at scales shorter than the measurements (Burrough 1983).

Variogram models were not fit to the data, so the nugget was estimated by fitting a line through the semivariance in the two shortest bins to the y-axis. The ratio between the extrapolated nugget and the overall variance was used as an estimate of the nugget ratio, here termed "nugget ratio estimate (NRE)" to differentiate it from a true nugget ratio (Logan, 2005).

A semi-spatial method to characterize the spatial variability of τ_∞ was the pit-to-plot ratio, (*PPR*) (Birkeland and Landry, 2002; Landry, 2002, Landry et al., 2004). *PPR* characterized the ability of a single pit to represent the results of the entire plot,

$$PPR = \frac{Pit_{represent}}{Pit_{total}} \tag{6}$$

where $Pit_{represent}$ was the total number of representative pits, and Pit_{total} was the number of pits within the plot, in this case the five main pits. If more pits were statistically representative of the plot, *PPR* was high and the plot was less spatially variable. Low *PPR* values indicated fewer representative pits and greater spatial variability. A pit was representative of the plot if there was no statistically significant difference between the results in a pit and the results of all the tests for a plot. The Wilcoxon Test was used to compare the individual pits to the pooled results. The Wilcoxon Test assumed that the data distributions were identical, but not necessarily normal. To increase the conservativeness of the test, results from all the main pits were pooled, and individual pits compared to the pooled result (Birkeland and Landry, 2002; Landry, 2002, Landry et al., 2004).

2.3. Detecting changes in spatial variability

After analyzing the spatial patterns of individual plots, temporal change between the plots was assessed by comparing the statistical measures of a plot and the one sampled prior. Indicators of increasing spatial variability were decreases in the range of the variograms, an increase in the NRE,

and a decrease in *PPR* (fewer representative pits). Increasing variogram range, decreasing NRE, and increasing *PPR* would indicate increasing spatial uniformity. An increasing range indicated an increase in the distance at which test results were spatially autocorrelated.

3. RESULTS

3.1. Spanky's Plot

A layer of near surface facets topped with surface hoar developed at the site prior to 22 January 2004. Snowfall began on 23 January, with approximately 25 cm of snow on top of the surface hoar by 24 January. We sampled the alleys on 26 January 2004, as the weather cleared, and Plot 1 three days later (Table 1). We were able to conduct additional tests while sampling Plot 1, for a total of 89 shear frame tests. Plot 2 was sampled on 5 February, Plot 3 on 12 February, and Plot 4 on 20 February. Slab properties, weak layer strength, and per-day changes are summarized for the five sample days (Table 1; Figure 3).

There was no significant linear trend in the τ_∞ data of the Alley sample (Table 2; $p = 0.32$). Since no trends existed across the site, we assumed similar initial conditions in all four plots. The increase in τ_∞ was significant ($p < 0.001$) between the Alleys and Plot 1. The Plot 1 variogram indicated spatial autocorrelation at short distances (Figure 4) with a range of 0.5 m and a NRE of 0 (or 0.25 if calculated from the 1st and 3rd bins). The point pairs at distances less than 0.5 m consisted of the additional tests conducted in Plot 1, which provided short pair distances and shorter minimum distances between tests than the other plots. On Plot 1, the shear frame test with the lowest shear strength was within 0.5 m of one of the tests with the highest shear strengths, further suggesting spatial autocorrelation only at short distances. Such close proximity of very high and very low test results has been noted in other studies (e. g. Landry, 2002). One pit was not representative of plot τ_∞ (*PPR* = 0.8; Figure 5).

Variograms for Plots 2, 3, and 4 had nugget ratio estimates greater than 0.45 and indicated little spatial autocorrelation. Corresponding with the variograms, all pits were representative of Plots 2, 3, and 4 (*PPR* = 1). The spatial distribution of τ_∞ was apparently random across the three plots.

Although we remained cautious about our spatial analysis of the four plots given the quality of the variograms, the nugget estimate increased from Plot 1 to Plot 2, reflecting the lack of tests at close distances in Plot 2 and decreasing autocorrelation of τ_∞. *PPR* increased, with all pits representative of Plot 2. Taken together, the changes suggest that spatial autocorrelation may have decreased in the week between the sampling of Plot 1 and 2.

Significant strengthening occurred between the all of the plots (Table 1; Figure 3). The rate of strengthening was highest early in the sampling, and that rate decreased through time. The decrease in the rate of strengthening as the surface hoar aged is consistent with previous studies and experience (Chalmers and Jamieson, 2001; Jamieson and Johnston, 1999; Jamieson and Schweizer, 2000; McClung and Schaerer, 1993; Tremper, 2001). The QCV of strength varied only slightly, ranging from 0.091 to 0.107 for all the plots except Plot 2 (Table 1). Essentially, the relative spread of the data remained constant, a result consistent with Chalmers and Jamieson (2001). However, the variance increased significantly each sampling day, demonstrating an increase in the absolute spread of τ_∞ as the layer aged.

3.2. Lionhead Plot Characteristics

An extensive layer of surface hoar formed throughout the Rocky Mountains in the middle of January 2004. Observations near the Lionhead site on 22 January recorded two layers of surface hoar with grains up to 55 mm, separated by a thin layer of precipitation particles (Figure 6). Snowfall on 24-26 January buried and preserved the surface hoar layers. A widespread avalanche cycle on the layer occurred at the end of January.

We sampled the Alleys on 7 February. Avalanches had run adjacent to the site, probably during the 26 January avalanche cycle. Deposition had come within 3 m of the outside margins of Plots 2 and 3. The field crew was concerned that the avalanches had collapsed the surface hoar layer across the site, but crystals in both layers of surface hoar were upright in pits dug around the site during the initial setup.

One quarter of the way into the sampling of the alleys, the upper surface hoar layer collapsed. The lower surface hoar layer remained upright and intact (Figure 7). A tensile crack opened up across

the site, arcing from the corner of the cross-slope alley, up and across the upper two plots to the top of the up-slope alley (Figure 8). We continued the Alley sample after the collapse. Prior to the collapse, it was hard to determine which of the surface hoar layers fractured in the shear frame tests, because tests disrupted both layers. After the collapse, shear frame testing caused fractures on the upper, collapsed layer. The shear frame measurements before and after the collapse, and their implications, are discussed in detail in another paper (Birkeland, et al., in prep.).

The median τ_∞ of un-collapsed tests was 1103 Pa, and the median τ_∞ decreased dramatically to 427 Pa for collapsed tests ($p < 0.001$; Table 4; Figure 9). Two additional measurements above the tensile crack at the upslope end of the alley were more than 400 Pa stronger than tests below the crack, 0.5 m away (Figure 9). Over the 4.5 hr after the collapse, τ_∞ increased significantly and approximately linearly (Birkeland, et al., in prep.). Other observers have noted more rapid shear strength increases a weak layer collapse (Kronholm 2004), but this was not the case with this layer.

It was not possible to determine from the Alleys if any site-wide trends existed, or if the plots were similar. The number of pre-collapse tests was insufficient, and concentrated within the lower limb of the up-slope alley, and the post collapse results changed through the sample period.

We sampled the upper right plot on the following day, 8 February (Figure 10), because we wanted to compare collapsed and un-collapsed tests. There was no significant difference between the collapsed and un-collapsed areas ($p = 0.061$). The QCV decreased dramatically and the difference in variance was significant ($p_T < 0.001$), indicating a decrease in both the relative and absolute spread of τ_∞ as the difference between the two areas disappeared. Similar to tests in the Alley prior to the collapse, it was difficult to determine in which of the two surface hoar layers the shear frames failed.

There was a significant ($p = 0.002$) linear trend across Plot 1, but it explained too little of the variance ($R^2 = 0.005$) to affect the variogram analysis (Table 2). The trend reflected the location of the un-collapsed tests in the upper portion of the plot. The Plot 1 variogram had a range just under 2 m, within the intra-pit distance. This relatively short range meant all the spatial autocorrelation occurred within the individual pits. Because there was no significant spatial structure at the inter-pit distances, any pit represented the plot. This was reflected in *PPR*, with all pits representative of Plot 1.

Plot 2 was sampled 17 February. Snowfall in the week between sampling obscured all traces of the tensile crack. Although the crack was somewhat symmetrical around the up-slope alley, there were not obvious differences in shear strength or test behavior to differentiate collapsed or un-collapsed tests. The increase in τ_∞ between Plot 1 and 2 were significant ($p < 0.001$; Table 3). As with the Spanky's site, we observed little difference in the relative spread of τ_∞ as measured by the QCV. However, the variance differed significantly ($p < 0.001$) as the layer strengthened and the absolute spread increased.

There was a significant ($p < 0.001$, R2 = 0.239; Table 2) linear trend across Plot 2, reflecting the location of the tensile crack, with tests below the tensile crack tending to be stronger than tests above (Figure 9). The force of the collapse may have compacted the lower surface hoar layer, thus increasing the contact and rate of bonding between grains. The variogram of the de-trended data had a NRE of 0.7, indicating very little spatial autocorrelation. The *PPR* also reflected the location of the tensile crack, with the weaker, non-representative pit in the portion of the plot that would have been un-collapsed. The increase in variogram range between Plot 1 and 2 suggested a decrease in spatial variability, as did the decrease in *PPR* and slight increase in the QCV of shear strength.

Plot 3 was sampled on 24 February, and had a significant linear trend ($p < 0.001$; $R^2 = 0.123$, Table 2). Shear strength tended to be lower at the bottom of the plot than at the top. After removing the trend, the NRE was 0.5, and the variogram indicated little spatial autocorrelation, preventing assessments of changes in spatial variability. *PPR* indicated that all pits were representative of Plot 3.

Plot 4 was sampled on 2 March. A significant linear trend existed within the shear strength data, but explained too little of the variance ($p = 0.003$, $R^2 = 0.063$, Table 2) to affect the variogram calculation. The variogram for Plot 4 (Figure 11) was similar to a pure nugget variogram, indicating that very little spatial autocorrelation existed. The lack of spatial autocorrelation indicated by the variogram suggests uniform conditions across the plot. Though three of the four pits were representative of plot strength, the pit with the highest median pit strength was not ($p = 0.019$).

In summary, results from the Lionhead plot are similar to those from Spanky's. Shear strength increased significantly between each plot, and the rate of increase decreased by the last sampling day (Table 3). Strengthening rates were within the range of those reported by others (i.e., Jamieson and

Johnston, 1999), but were on the low end of those rates. Consistent with surface hoar layers investigated by Chalmers and Jamieson (2001), the relative spread, as measured by the QCV, remained relatively consistent through the sampling period. The absolute spread increased significantly between sampling days.

4. DISCUSSION AND IMPLICATIONS

4.1. Spatial Structure

Significant linear trends existed at all four of Lionhead plots, but only the trend for Plots 2 and 3 explained sufficient variability for removal; no significant linear trends existed at any of the Spanky's sites. In contrast, Kronholm and Schweizer (2003) found significant trends in 6 of 16 plots sampled. One difference between the current and previous studies was the wind-sheltered location of the study sites. Kronholm and Schweizer (2003) and Kronholm (2004) used alpine sites, and attributed the slope-scale trends to effects of the wind. If wind is a primary cause of the slope-scale trends, our wind-sheltered sites would greatly reduce the resultant trends. Further, slope angles varied considerably on some of Kronholm's slopes (as much as 24° at one site). This would also help to explain some of the slope scale trends, with the trends reflecting changes in the underlying terrain. In contrast, the slope angles of our two study sites varied less than 7°.

The variograms indicated little spatial autocorrelation, and they had large nugget ratio estimates. There may be several reasons for this: 1) the sampling array was not sufficient to characterize a short autocorrelation length of shear strength 2) the sites were so uniform that there was little autocorrelation to measure, and 3), there could be considerable fundamental error in the shear frame test.

If the spatial correlation of shear strength occurred at distances less than 1 m, the sampling array used at all but one plot would fail to capture the spatial pattern. The sampling array was designed to capture spatial autocorrelation at distances of several meters. Semivariance at the shortest distances on the Spanky's Plot 1 variogram, where additional tests were spaced closer than 0.5 m, indicated autocorrelation at distances less than 1 m over the slope. Additional support for

autocorrelation at short distances came from experience through the field season. If we felt a test was faulty, a second test was often placed as closely as possible to the first test. Unless the initial fault was due to an improperly prepared test, the second result tended to be more similar to the "faulty" test than two tests at the standard distance of 0.5 m.

There may have been little autocorrelation to measure because we sought out uniform slopes. If the snowpack was perfectly uniform, the expected variogram would be pure nugget. Several of our variograms contained such high nugget ratios that they could be considered pure nugget. Making a similar set of measurements over non-uniform slopes might indicate correlation lengths related to changes in topography, vegetation, or wind effects that could not be observed across our study sites.

There might be large fundamental error in the shear frame test that would result in irreducibly large NREs (Myers, 1997). The measurement support, or size, can directly influence the fundamental error of sampling (Myers, 1997). Shear frame measurements, with an area of 0.025 m^2, could contain considerable fundamental error. Larger measurement support, such as compression tests or rutschblocks, could reduce the potential fundamental error. We sought to minimize operator error, both in test preparation and placement, but human error would contribute to the fundamental error. However, our coefficients of variation for individual pits (10-12 shear frame tests) ranged from 6% to 50%, which compares favorably with the coefficients of variation ranging from 3% to 66% (with a mean of 15%) reported by Jamieson and Johnston (2001) for 809 sets of shear frame measurements.

4.2. Temporal Change

Median τ_∞ did change significantly between all plots (Figure 3, Figure 10). The buried surface hoar layers strengthened through time, and the rate of strengthening decreased as the layer aged. The rate of strengthening, and decreasing rate with layer age, is similar to rates reported by Jamieson and Johnston (1999), and Jamieson and Schweizer (2000). Of our two layers, Lionhead is the most similar to the layers observed by Jamieson and Schweizer (2000), with rates between 48 and 37 Pa d^{-1} (Table 3), comparable to their reported rates of 55 and 25 Pa d^{-1}. The initial rate of strengthening at Spanky's was more rapid, then decreased dramatically between Plot 3 and 4.

Also consistent with previous work was the increase in absolute spread as median τ_∞ increased, but only small changes in the relative spread (Chalmers and Jamieson, 2001). The CV changed less than 7% on one layer, and less than 25% on the second surface hoar layer discussed by Chalmers and Jamieson (2001). The largest change in QCV we observed was between Spanky's Plots 2 and 3, which would be an approximately 5% change in CV. Although the relative spread remained similar, the absolute spread of τ_∞, as measured by the variance, increased as the layer aged. This suggests that some weaker areas of the snowpack might remain relatively weak while the overall strength of the slope increases. Further, this can happen even on relatively uniform slopes, and not just around topographic features. Our results reflect observations of experienced forecasters. As persistent weak layers age, predicting instability on those layers becomes increasingly difficult as the absolute spread of stability test results increases. This continues until the median and absolute variability in stability on the slope increases to the point that the overall slope is stable.

Changes in the spatial measures were more difficult to determine because the variograms were hard to interpret and *PPR* differed little between plots. At both sites, changes in spatial structure were strongest between Plots 1 and 2, because the variograms were interpretable. This suggested that the potential for changes in spatial structure was greatest when the shear strength was increasing most rapidly. The potential for changes in the spatial patterns then seemed to decrease as the layer aged, and the rate of strengthening slowed.

4.3. Pit-to-Plot Ratios

We anticipated that more pits might not be representative of the plot based on Landry (2002) and Landry et al., (2004). In that work, over one third of the pits were not representative of the plots, while in our study only 10% of the pits (4 pits out 40 total pits from 8 plots) were not representative of plot-wide τ_∞. Because *PPR* changed little between plots, it did not indicate a temporal trend.

The pit-to-plot analysis did allow us to examine the ability of a forecaster to extrapolate stability tests a short distance over uniform sites. On our two buried surface hoar layers, over relatively uniform slopes, τ_∞ could be reliably extrapolated for 17 m (the diagonal distance across the plot) from 90% of our pits. For an avalanche forecaster, the ability to extrapolate reliably is encouraging, and this result

contradicts some of Landry (2002) and Landry et al., (2004) research on similar slopes that utilized larger plots and a different stability test.

Several differences between this study and Landry (2002) and Landry et al., (2004) might explain the differences. First, our plots were about one fourth of the area of Landry's, with distances between pits about one fourth of the distance between Landry's pits. Spatial trends at scales that Landry's tests could pick up might be undetectable with our layouts. This would be especially true of slope-scale trends, which would cause much greater differences at the scale of Landry's study. The explanatory power of a significant linear trend could be relatively low at the size of our plots, but influence *PPR* at the size of Landry's plots (Logan, 2005).

Second, the type of test used was perhaps the most critical difference between the current study and Landry's work. Landry used the Quantified Loaded Column Test (Landry et al., 2001), which integrated slab characteristics into the test result. The shear frame test removed the slab from the test, and tested only the weak layer. This could account for some of the differences, especially if stronger trends were present in the slab than in the weak layer (Kronholm, 2004; Lutz, 2004).

5. CONCLUSIONS

We examined temporal changes in the spatial structure of shear strength of two buried surface hoar layers. By sampling adjacent plots, we followed the same layers through more than 3 weeks. Spatial structures were examined with geostatistical methods and pit-to-plot ratios.

At both sites, shear strength increased significantly between all sample days. The rate of strengthening decreased as the layers aged. We were able to capture the initial weakening after the upper layer collapsed at the Lionhead site, followed by relatively rapid strengthening over the sampling day. On the following day, there was little difference in shear strength between tests on the collapsed and un-collapsed layer (Table 4).

Spatial structure proved elusive. Only two plots, both at the Lionhead site, had significant trends across the plot. One trend was related to the collapse and tensile crack. The other trend was not related to any observable difference within the plot, but the plot may have been affected by prior

sampling of the plot up-slope. If our plots had been larger, slope-scale trends may have been easier to detect, but selecting uniform sites may reduce or eliminate any slope scale trends.

The variograms indicated little spatial autocorrelation after the first or second plot at each site. There was little relationship between shear frame measurements, suggesting that shear strength could be treated as a random variable, for these two layers, after more than 2 weeks after burial. We conducted additional shear frame tests at Spanky's Plot 1, spaced closer than the standard 0.5 m between test centers. The additional tests suggest that shear strength was autocorrelated at distances less than 1 m. Our standard sampling array would miss potential autocorrelation at that short distance. The short correlation length is consistent with previous experience, where adjacent strong and weak tests were measured (Landry et al., 2004)

Because the spatial analysis indicated little spatial structure, our analyses provided little indication of temporal changes in spatial variability. Our current challenge is to develop methods and techniques for adequately characterizing that variability and capturing those temporal changes.

ACKNOWLEDGEMENTS

Many thanks to Eric Lutz for all his help in the field in the summer and winter, for his assistance in organizing field days, and for his discussions on the ideas in this paper. We also thank Shannon Moore for his assistance in the field. Linda Bishop and Grant Estey facilitated site access. Two anonymous reviews provided constructive comments that improved the paper. This research was financially supported by National Science Foundation (Grant #BCS-0240310). Spencer Logan was partially supported by the Barry C. Bishop Scholarship for Mountain Research and the Department of Earth Sciences at Montana State University.

REFERENCES

Birkeland, K. W., and C. C. Landry. 2002. Changes in spatial patterns of snow stability through time. Proceedings of the 2002 International Snow Science Workshop, Penticton, British Columbia, Canada [CD-ROM].

Birkeland, K., K. Kronholm, and S. Logan. 2004. A comparison of the spatial structure of the penetration resistance of snow layers in two different snow climates. Proceedings of the International Symposium on Snow Monitoring and Avalanches, Manali, India, 3-11.

Birkeland, K.B., K. Kronholm, J. Schweizer, and S. Logan. In preparation. Field measurements of sintering after fracture of weak snowpack layers.

Blöschl, G., 1999. Scaling issues in snow hydrology. Hydrological Processes, 13(14-15): 2149-2175.

Burrough, P. A., 1983. Multiscale sources of spatial variation in soil .1: The application of fractal concepts to nested levels of soil variation. Journal of Soil Science 34 (3):577-597.

Chalmers, T.S. and Jamieson, J.B., 2001. Extrapolating the skier stability of buried surface hoar layers from study plot measurements. Cold Regions Science and Technology, 33(2-3): 163-177.

Conway, H. and Abrahamson, J., 1984. Snow Stability Index. Journal of Glaciology, 30(106): 321-327.

Cressie, N.A.C., 1993. Statistics for Spatial Data. Wiley Series in Probability and Mathematical Statistics. John Wiley and Sons, Chichester, 900 pp.

Föhn, P. M. B. 1987. The stability index and various triggering mechanisms. In Avalanche Formation, Movement, and Effects, eds. B. Salm and H. Gubler, 195-211: IASH-AISH.

Greene, E., K. W. Birkeland, K. Elder, G. Johnson, C. C. Landry, I. McCammon, M. Moore, D. Sharaf, C. Sterbenz, B. Tremper, and K. Williams. 2004. Snow, Weather, and Avalanches: Observational Guidelines for Avalanche Programs in the United States. 1st ed. American Avalanche Association, Pagosa Springs, 136 pp.

Jamieson, J.B. and Johnston, C.D., 1992. Snowpack characteristics associated with avalanche accidents. Canadian Geotechnical Journal 29, 862-866.

Jamieson, J.B. and Johnston, C.D., 1999. Snowpack factors associated with strength changes of buried surface hoar layers. Cold Regions Science and Technology, 30(1-3): 19-34.

Jamieson, J.B. and Johnston, C.D., 2001. Evaluation of the shear frame test for weak snowpack layers. Annals of Glaciology, 32: 59-69.

Jamieson, J.B. and Schweizer, J., 2000. Texture and strength changes of buried surface-hoar layers with implications for dry snow-slab avalanche release. Journal of Glaciology, 46(152): 151-160.

Kronholm, K., 2004. Spatial Variability of Snow Mechanical Properties with regard to Avalanche Formation, Doctoral Dissertation, Universitat Zurich, Zurich, 177 pp.

Kronholm, K. and Schweizer, J., 2003. Snow stability variation on small slopes. Cold Regions Science and Technology, 37(3): 453-465.

Kronholm, K., Schneebeli, M., and Schweizer, J., 2004. Spatial variability of penetration resistance in snow layers on a small slope. Annals of Glaciology 38: 202-208.

LaChapelle, E.R., 1980. The Fundamental Processes in Conventional Avalanche Forecasting. Journal of Glaciology, 26(94): 75-84.

Landry, C.C., 2002. Spatial variations in snow stability on uniform slopes: Implications for extrapolation to surrounding terrain. MS Thesis, Montana State University, Bozeman, 248 pp.

Landry, C., Birkeland K., Hansen K., Borkowski J., Brown R., and Aspinall, R., 2004. Variations in snow strength and stability on uniform slopes. Cold Regions Science and Technology, 39(2-3): 205-218

Lark, R.M., 2000. A comparison of some robust estimators of the variogram for use in soil survey. European Journal of Soil Science, 51(1): 137-157.

Logan, S. C., 2005. Temporal changes in the spatial patterns of weak layer shear strength and stability on uniform slopes. MS Thesis, Montana State University, Bozeman, 173 pp.

McClung, D.M., 2002. The elements of applied avalanche forecasting - Part I: The human issues. Natural Hazards, 26(2): 111-129.

McClung, D.M. and Schaerer, P., 1993. The Avalanche Handbook. The Mountaineers, Seattle, 271 pp.

Mock, C.J. and Birkeland, K.W., 2000. Snow avalanche climatology of the western United States mountain ranges. Bulletin of the American Meteorological Society, 81(10): 2367-2392.

Myers, J.C., 1997. Geostatistical Error Management: quantifying uncertainty for environmental sampling and mapping. Van Nostrand Reinhold, New York, 571 pp.

Neter, J., Kutner, M. H., Nachtsheim, C. J., Wasserman., W., 1996. Applied Linear Statistical Models. 4th ed. WCB/McGraw Hill, Boston, 1408 pp.

Schweizer, J., Jamieson, J.B., 2001. Snow cover properties for skier-triggering of avalanches. Cold Regions Science and Technology 33, 207-221.

Schweizer, J., Jamieson, J.B. and Schneebeli, M., 2003. Snow avalanche formation. Reviews of Geophysics, 41(4), 1016.

Spiegel, M.R. and Stephens, L.J., 1999. Schaum's outline of theory and problems of statistics. Schaum's outline series. McGraw-Hill, New York, 538 pp.

Stewart, K. and Jamieson, B., 2002. Spatial variability of slab stability in avalanche start zones. Proceedings of the 2002 International Snow Science Workshop, Penticton, British Columbia, Canada [CD-ROM].

Tremper, B., 2001. Staying Alive in Avalanche Terrain. The Mountaineers, Seattle, 284 pp.

Webster, R. and Oliver, M.A., 2001. Geostatistics for Environmental Scientists. Statistics in Practice. John Wiley and Sons, Chichester, 271 pp.

Table 1. Characteristcs of the slab and weak layer for each plot at the Spanky's site, and rates of change between samples.

	Alley	Plot 1	Plot 2	Plot 3	Plot 4
Date sampled	26 Jan	29 Jan	5 Feb	12 Feb	20 Feb
Median slab thickness (cm)	45	34	47	66	72
QCV of slab thickness	0.018	0.002	0.011	0.023	0.014
Median slab density (kg m^{-3})	98	129	157	148	183
QCV of slab density	0.041	0.034	0.015	0.024	0.011
Median shear strength (Pa)	479	682	1070	1376	1466
QCV of shear strength	0.091	0.093	0.060	0.096	0.107
Number of shear frames	48	89	74	74	74

	Alley and Plot 1	Plots 1 and 2	Plots 2 and 3	Plots 3 and 4
Number of days between:	3	7	7	8
Change in median slab thickness (cm d^{-1})	-4	2	3	1
Change in median slab density (kg m^{-3} d^{-1})	10.3	4	-1.3	4.4
Change in median shear strength (Pa d^{-1})	**68**	**55**	**44**	**12**
Significance, change in shear strength	< 0.001	< 0.001	< 0.001	< 0.001
Significance, difference in variance	< 0.001	< 0.001	< 0.001	< 0.001

Table 2. Significance, correlation, and coefficients of the linear trends in shear strength at both Spanky's and Lionhead sites. Trends that were significant and explained more than 10% of the variability are indicated in bold. The significant trend in the Lionhead Alley was related to the collapse of the weak layer during sampling.

		p-value	R^2	a_1	a_2	a_3
Spanky's	Alley	0.335	0.047	476	2.01	-0.93
	Plot 1	0.293	0.053	732	-479	-2.22
	Plot 2	0.192	0.037	1170	-3.75	-0.59
	Plot 3	0.240	0.009	1562	0.21	-9.86
	Plot 4	0.216	0.216	1767	-4.28	-11.42
Lionhead	Alley	**< 0.001**	**0.174**	**945**	**3.25**	**-22.81**
	Plot 1	0.002	0.005	776.16	7.66	-3.15
	Plot 2	**< 0.001**	**0.239**	**1720**	**20.66**	**-23.43**
	Plot 3	**< 0.001**	**0.128**	**1440**	**2.27**	**28.63**
	Plot 4	0.003	0.063	2410	-23.92	9.55

Table 3. Characteristcs of the slab and weak layer for each plot at the Lionhead site, and rates of change between samples.

	Alley	Plot 1	Plot 2	Plot 3	Plot 4
Date sampled	7 Feb	8 Feb	17 Feb	24 Feb	2 Mar
Median slab thickness (cm)	53.25	53	61	61	86
QCV of slab thickness	0.011	0.009	0.008	0.016	0.006
Median slab density (kg m^{-3})	151	158	182	213	209
QCV of slab density	0.051	0.021	0.018	0.030	0.011
Median shear strength (Pa)	504	886	1300	1581	1912
QCV of shear strength	0.440	0.125	0.130	0.108	0.093
Number of shear frames	50	74	74	74	74

	Alley and Plot 1	Plots 1 and 2	Plots 2 and 3	Plots 3 and 4
Number of days between:	1	9	7	9
Change in median slab thickness (cm d^{-1})	-0.25	0.89	0.00	2.78
Change in median slab density (kg m^{-3} d^{-1})	7	.26	4.5	-0.4
Change in median shear strength (Pa d^{-1})	**362**	**48**	**40**	**37**
Significance, change in shear strength	<0.001	<0.001	<0.001	<0.001
Significance, difference in variance	< 0.001	< 0.001	< 0.001	< 0.001

Table 4. Comparison of tests made in the collapsed and un-collapsed areas of the Lionhead Alley and Plot 1

	Alley	**Plot 1**
Median shear strength, un-collapsed (Pa)	1103	931
Median shear strength, collapsed (Pa)	427	854

Figure 1. Map of the study site locations in southwestern Montana, USA.

Figure 2. Location of stability tests (squares) for the alley and all four plots. Plot numbers for Spanky's and Lionhead (in parentheses) are indicated.

Figure 3. Boxplots of shear strength for each plot at the Spanky's site. Dotted lines indicate medians, boxes the interquartile range, and whiskers extend to 0.05 and 0.95 quantiles.

Figure 4. The variogram for Spanky's Plot 1, the only variogram to indicate much spatial autocorrelation. The thin line indicates the NRE, using the first and third bin.

Figure 5. Box plot of the shear strength in individual pits in Spanky's Plot 1. The only pit not representative of the plot was Pit 1 ($p = 0.05$), though there was some evidence that Pit 3 was not representative ($p = 0.07$). Dotted lines indicate medians, boxes the interquartile range, whiskers extend to 0.05 and 0.95 quantiles, and circles indicate outliers. The pooled results are indicated on the right, labeled "All pits."

Figure 6. A close-up photo of the double surface hoar layers at the Lionhead site, taken prior to the collapse. The ruler is marked in centimeters.

Figure 7. Close-up photo of the tensile crack and collapsed surface hoar, taken shortly after the collapse. The ruler is marked in centimeters.

Figure 8. The tensile crack at the Lionhead site (thin line). Plots were sampled in the order numbered.

Figure 9. Shear strength of the Lionhead Alley tests, in measurement order. Tests made after the collapse are in white. The collapse occurred between tests 15 and 16, and the white bars indicate

tests conducted on the collapsed layer. Tests 25 and 26 were made above the tensile crack, just upslope of tests 23 and 24.

Figure 10. Boxplots of shear strength for each plot at the Lionhead site. Dotted lines indicate medians, boxes the interquartile range, and whiskers extend to 0.05 and 0.95 quantiles.

Figure 11. The variogram for Lionhead Plot 4, a pure nugget variogram. The thin line indicates the NRE.

Figure 1.

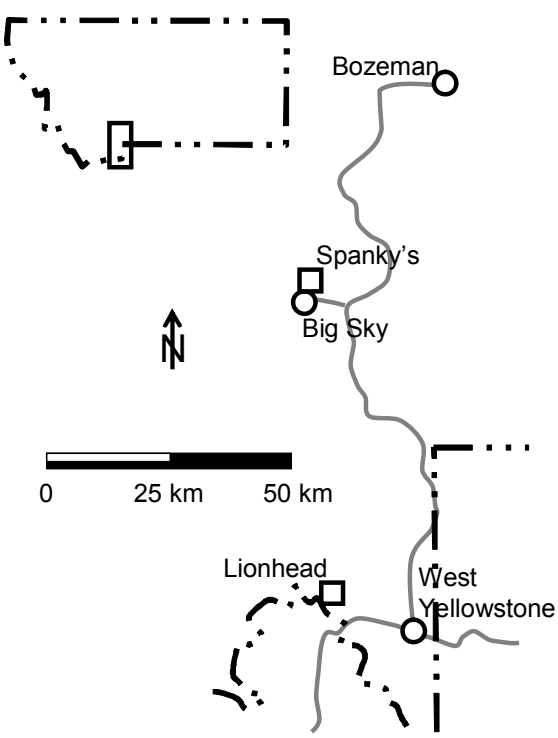
Bozeman
Spanky's
Big Sky
N
0
25 km
50 km
Lionhead
West
Yellowstone

Figure 2.

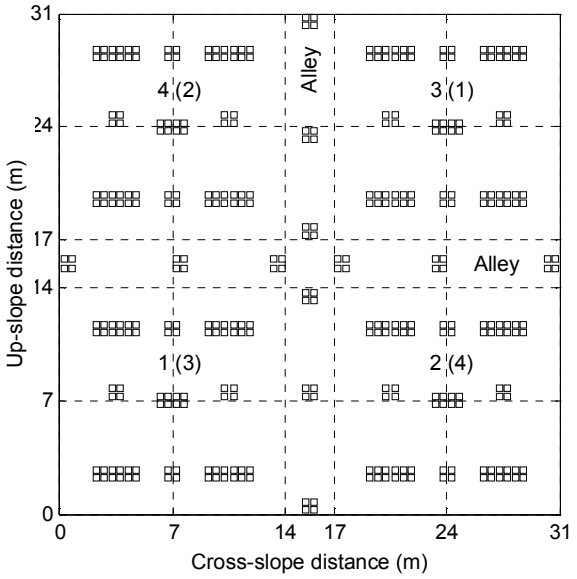
31
24
17
14
7
0
0
7
14
17
24
31
Up-slope distance (m)
Cross-slope distance (m)
Alley
Alley
4 (2)
3 (1)
1 (3)
2 (4)

Figure 3.

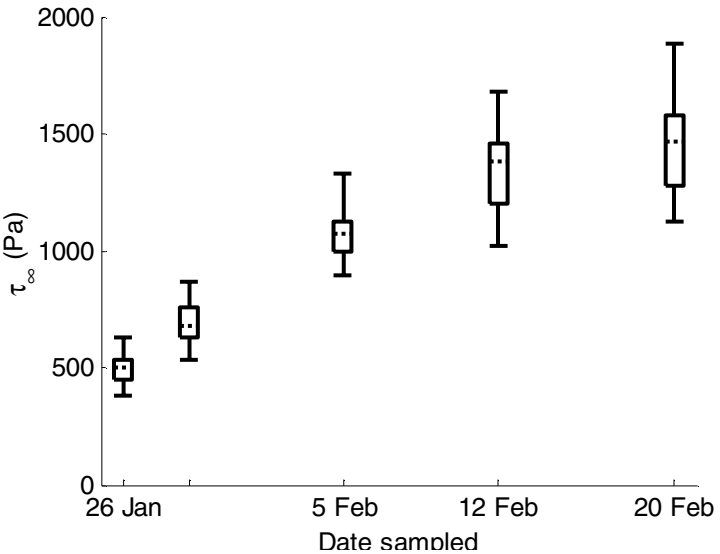

Figure 4.

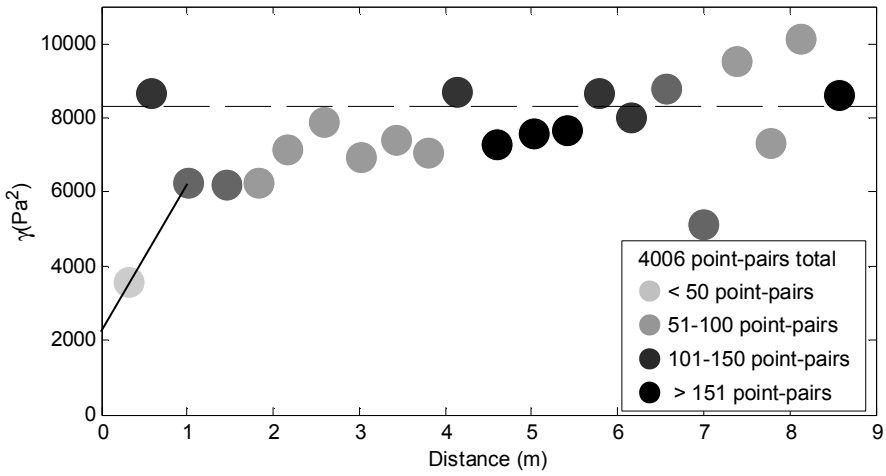
10000
8000
6000
4000
2000
0
γ(Pa²)
0
1
2
3
4
5
6
7
8
9
Distance (m)
4006 point-pairs total
< 50 point-pairs
51-100 point-pairs
101-150 point-pairs
> 151 point-pairs

Figure 5.

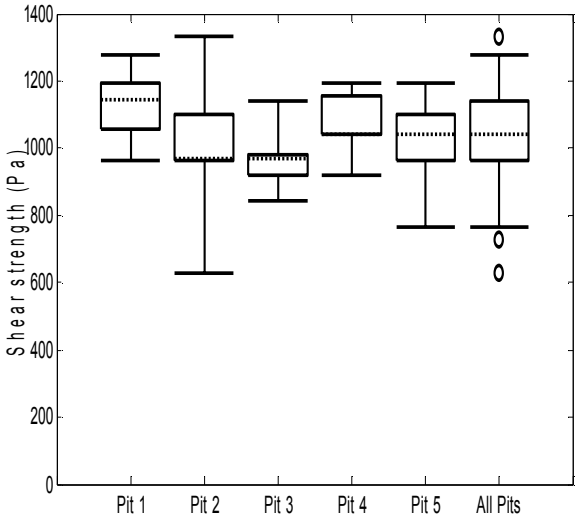
Shear strength (Pa)
1400
1200
1000
800
600
400
200
0
Pit 1
Pit 2
Pit 3
Pit 4
Pit 5
All Pits

Figure 6.

Figure 7.

Figure 8.

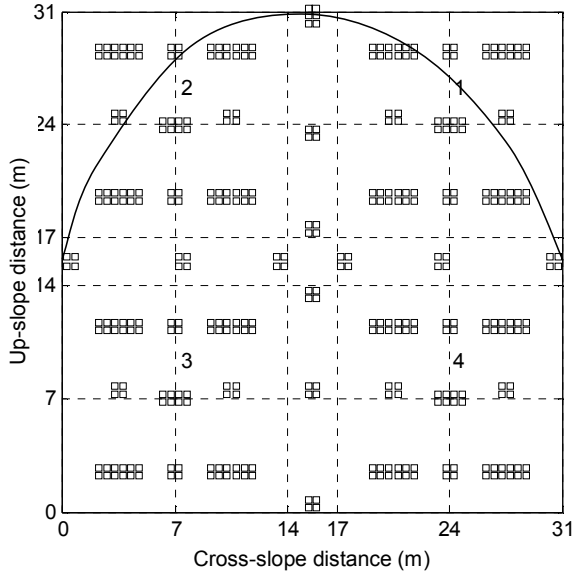
31
24
17
14
7
0
Up-slope distance (m)
0
7
14
17
24
31
Cross-slope distance (m)
1
2
3
4

Figure 9.

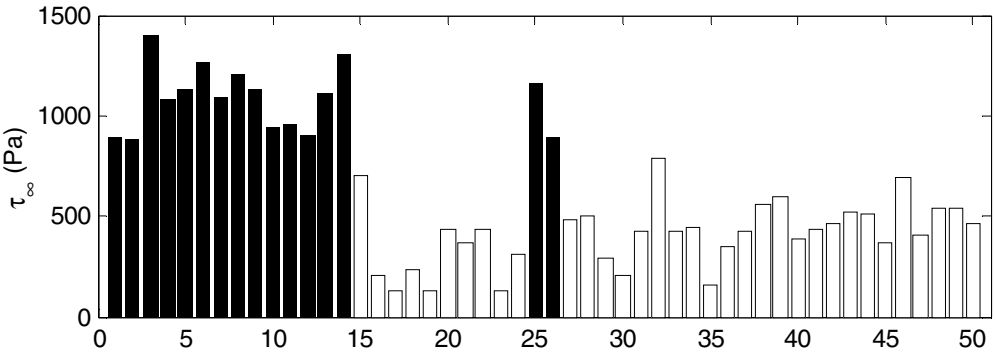

Figure 10.

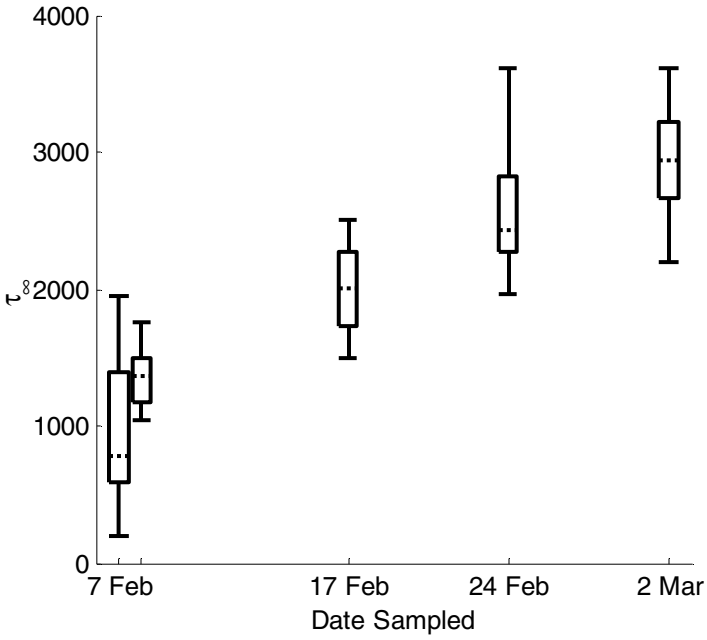
4000
3000
2000
1000
0
τ_s
7 Feb
17 Feb
24 Feb
2 Mar
Date Sampled

Figure 11.

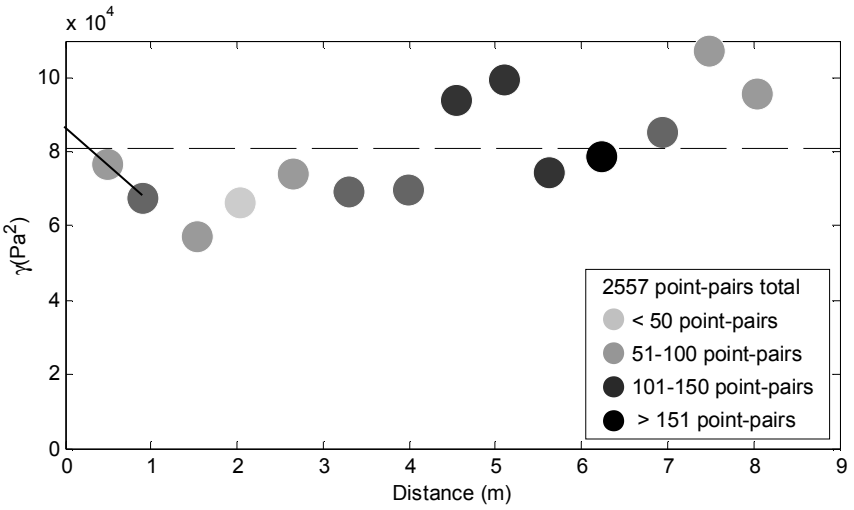
x 10^4
10
8
6
4
2
0
γ(Pa^2)
0
1
2
3
4
5
6
7
8
9
Distance (m)
2557 point-pairs total
< 50 point-pairs
51-100 point-pairs
101-150 point-pairs
> 151 point-pairs